Global phase diagram and momentum distribution of single-particle excitations in Kondo insulators

J. H. Pixley, Rong Yu, Silke Paschen, and Qimiao Si

Phys. Rev. B **98**, 085110 — Published 7 August 2018

DOI: 10.1103/PhysRevB.98.085110

Global Phase Diagram and Momentum Distribution of Single-Particle Excitations in Kondo Insulators

J. H. Pixley,[1] Rong Yu,[2,3] Silke Paschen,[4] and Qimiao Si[5]

[1] *Condensed Matter Theory Center and Joint Quantum Institute, Department of Physics, University of Maryland, College Park, Maryland 20742- 4111 USA*
[2] *Department of Physics, Renmin University of China, Beijing, 100872, China*
[3] *Department of Physics and Astronomy, Collaborative Innovation Center of Advanced Microstructures, Shanghai Jiaotong University, Shanghai 200240, China*
[4] *Institute of Solid State Physics, Vienna University of Technology, Wiedner Hauptstraße 8-10, 1040 Vienna, Austria*
[5] *Department of Physics & Astronomy, Rice University, Houston, Texas, 77005, USA*

(Dated: June 10, 2016)

Kondo insulators are emerging as a simplified setting to study both magnetic and insulator-to-metal quantum phase transitions. Here, we study the half-filled Anderson lattice model defined on a magnetically frustrated Shastry-Sutherland geometry. We determine a "global" phase diagram that applies to both the local-moment and intermediate-valence regimes. This provides the theoretical basis for understanding how tuning a Kondo insulator by external parameters can close its hybridization gap, liberate the local-moment spins from the conduction electrons, and lead to a magnetically correlated metal. We also calculate the momentum distribution of the single-particle excitations in the Kondo insulating state, and show how Fermi-surface-like features emerge as a precursor to the actual Fermi surfaces of the Kondo-destroyed metals. The implications for an incipient Fermi surface and quantum phase transitions of Kondo insulators including SmB_6 are discussed.

PACS numbers: 71.10.Hf, 71.27.+a, 75.20.Hr

Quantum criticality in the vicinity of antiferromagnetic order is of interest to a variety of strongly correlated electron systems [1]. Heavy fermion systems occupy a special place in this context [2, 3]. These systems are typically described by a Kondo lattice model, which contains a lattice of local-moment spins coupled to a band of conduction electrons. Antiferromagnetic (AF) quantum critical points (QCPs) have been identified in a host of heavy fermion metals. Experimental studies at such QCPs [4–7] have provided evidence for a Kondo-destruction local QCP [8–10], across which the Fermi surface jumps from "large" (incorporating the f-electrons) to "small" (excluding the f-electrons). Experimental efforts have also been devoted to heavy fermion metals that allow a systematic tuning of inherent quantum fluctuations, through magnetic frustration [11–15], dimensionality [16], or other means [17–19], which shed new light on the emergence of novel phases. Theoretical considerations of such effects have advanced a global phase diagram [20–23].

Such developments in heavy fermion metals naturally lead one to ask whether and how novel phases and their transitions can be realized in Kondo insulators [24]. Such insulating states arise when the filling is commensurate and the chemical potential falls in the middle of a hybridization gap [25, 26]. If, by analogy with the case of the heavy fermion metals, an external parameter such as pressure, magnetic field, or doping tunes the system across a Kondo-destruction transition, the gap of the Kondo insulator will close. At the same time, the local-moment spins will be liberated from the conduction electrons, thereby yielding magnetic states in which the spin-rotational invariance is either spontaneously broken (*e.g.*, an AF order) or preserved (a valence-bond solid or a spin liquid). While these types of qualitative considerations have led to a proposed global phase diagram for Kondo insulators [27], systematic theoretical studies have yet to be performed. In addition, the case of mixed valency that is thought to be relevant for many Kondo insulators has never been considered in this context.

Studies along this direction are also important to understand the on-going experiments on Kondo insulators [24], which in recent years have been particularly fueled by the search for topological Kondo insulating states [28] in SmB_6 and related systems. Several developments have in particular motivated the present work. First, recent experiments [29] in pressurized SmB_6 have provided evidence for quantum criticality of a transition from a Kondo insulator to an antiferromagnetic metal [30, 31]. Second, torque magnetometry measurements have observed a de Haas-van Alphen signal in SmB_6 [32–34], raising the exciting possibility that the Kondo insulator state harbors an incipient Fermi surface of the same size as the (small) Fermi surface of LaB_6 [33, 34]. Third, there is growing experimental evidence that doping drives a Kondo insulator through a quantum critical regime into an AF metal, as in CeNiSn (doped with Pt, Pd, and Cu) [35]. Finally, there are emerging signatures for quantum criticality in several Kondo insulating compounds, including CeM_2Al_{10} (where M=Fe, Ru, Os) [36] and tentatively $CeRu_4Sn_6$ [37], suggesting that they are already in proximity to a QCP. These developments have

made quantum phase transitions in Kondo insulators to be of both fundamental and topical interest. Thus it is important to construct a generic theory for how Kondo insulator systems are tuned across various phase transitions, and how such transitions influence the electronic properties of the Kondo insulating state.

In this Letter, we study the periodic Anderson model (PAM) at half filling. In order to concretely study the effect of tuning quantum fluctuations of the local-moment magnetism, we focus on the model defined on the geometrically frustrated Shastry-Sutherland lattice. We are able to, for the first time, i) map out the global phase diagram from concrete theoretical calculations in well-defined models; ii) assess the robustness of the global phase diagram against non-integer f-electron valence (as are relevant for SmB_6); and iii) determine Fermi-surface-like features in the single-particle excitations of the Kondo insulating state for both mixed and integer valences.

The PAM model is written as

$$H = \sum_{(i,j),\sigma} t_{ij}(c^\dagger_{i\sigma}c_{j\sigma} + \text{h.c.}) + \sum_{(i,j)} J_{ij}\mathbf{S}_i \cdot \mathbf{S}_j + H_{mix} \quad (1)$$

where $c^\dagger_{i\sigma}$ creates a conduction electron of spin σ at site i, (i,j) denotes neighboring bonds, t_{ij} is a hopping strength , and J_{ij} is an RKKY interaction between the f-electron moments, and $\mathbf{S}_i = d^\dagger_{i\alpha}(\boldsymbol{\sigma}_{\alpha\beta}/2)d_{i\beta}$. H_{mix} is given by

$$H_A = \epsilon_d \sum_{i,\sigma} n^d_{i,\sigma} + U\sum_i n^d_{i,\uparrow}n^d_{i,\downarrow} + V\sum_{i,\sigma}\left(c^\dagger_{i\sigma}d_{i\sigma} + \text{H.c.}\right). \quad (2)$$

We have introduced $n^a_{i,\sigma} = a^\dagger_{i\sigma}a_{i\sigma}$, and we focus on the $U \to \infty$ limit, which allows for a representation, $d_{i\sigma} = f_{i\sigma}b^\dagger_i$, in terms of a spinon ($f_{i\sigma}$) and a slave boson ($b_i$) that are subject to the constraint $b^\dagger_i b_i + \sum_\sigma f^\dagger_{i\sigma}f_{i\sigma} = 1$ [38]. The condition for half filling is $n_d + n_c = 2$, where $n_d = \frac{1}{N_{site}}\sum_{i,\sigma}\langle n^d_{i\sigma}\rangle$ and $n_c = \frac{1}{N_{site}}\sum_{i,\sigma}\langle n^c_{i\sigma}\rangle$ are the fillings of the f- and conduction electrons, respectively. The on-site energy ϵ_d is variable to cover both the intermediate valence ($n_d < 1$) and local moment ($n_d \to 1$) regimes. The Kondo lattice model (KLM) is similarly defined and represented (see the Supplementary Material [39]).

For the Kondo lattice case away from half-filling, the global phase diagram of heavy fermion metals have been studied [23, 40, 41]. In this work, we consider the PAM away from integer valence.

Global phase diagram: We consider the two-dimensional (2D) PAM on the SSL geometry. It contains J_1 and J_2, the nearest neighbor (NN) and next nearest neighbor (NNN) RKKY interactions, respectively, and t_1 and t_2, the corresponding hoppings.

An important advantage of our treatment is that the large-N limit (where N corresponds to the generalization of spin degeneracy from SU(2) to SU(N)) properly captures the valence bond solid (VBS) phase of the SSL Heisenberg model [42, 43]. To study the magnetic state in the physical case of $N = 2$, we follow the general procedure of Hubbard-Stratonovich decouplings [44]: with guidance by the quantum magnetism effect of the SSL Heisenberg model, we introduce a parameter x to weight the decoupling of the Heisenberg interaction into the bond spin-singlet and AF channels, $D_{ij} = \sum_\sigma f^\dagger_{i\sigma}f_{j\sigma}$ and $\mathbf{S}_i = f^\dagger_{i\alpha}(\boldsymbol{\sigma}_{\alpha\beta}/2)f_{i\beta}$, respectively. The criterion is that the AF order is accompanied by nonzero singlet correlations, and this happens in the range $0.6 < x < 0.8125$ [23].

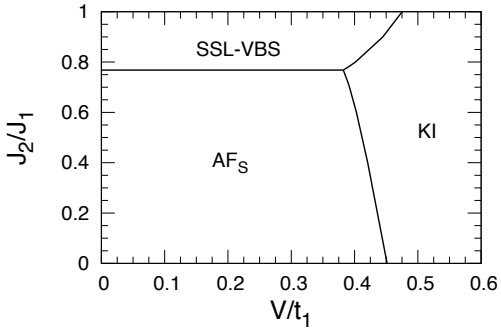

FIG. 1. Global phase diagram of Kondo insulators: Zero temperature phase diagram as a function of frustration (J_2/J_1) and hybridization strength (V/t_1) for the PAM, for half filling $n_d + n_c = 2.0$, $t_2/t_1 = 0.25$ and $\epsilon_d/t_1 = -0.5$. The phases and their transitions are described in the main text.

This procedure leads to

$$H_{MF} = C_{mix} - \sum_i \left[(b^*_i c^\dagger_{i\sigma}f_{i\sigma} + \text{h.c.}) + \tilde{\lambda}_i f^\dagger_{i\sigma}f_{i\sigma}\right] \quad (3)$$
$$+ \sum_{(i,j)}\left[(t_{ij}c^\dagger_{i\sigma}c_{j\sigma} - Q^*_{ij}f^\dagger_{i\sigma}f_{j\sigma} + \text{h.c.}) + \tilde{J}_{ij}2\mathbf{M}_i \cdot \mathbf{S}_j\right]$$

where the sum over σ is implied, and we have defined $\tilde{J}_{ij} = (1-x)J_{ij}$. We have $C_{mix} = C_A + \sum_{(i,j)}(2|Q_{ij}|^2/(xJ_{ij}) - \tilde{J}_{ij}\mathbf{M}_i \cdot \mathbf{M}_j)$, where $C_A = \sum_i \lambda_i\left(|b_i|^2 - 1\right)$, $\tilde{\lambda}_i = \lambda_i + \epsilon_d$ and the hybridization is $b_i = V\langle\sum_\sigma c^\dagger_{i\sigma}f_{i\sigma}\rangle/\lambda_i$. The Hubbard-Stratonovich parameters in the resonating valence bond singlet channel are $Q_{ij} = xJ_{ij}\langle D_{ij}\rangle/2$ and the AF order parameter is $\mathbf{M}_i = \langle\mathbf{S}_i\rangle$ [with an ordering wave vector $\mathbf{Q} = (\pi,\pi)$]. For definiteness, we show the results for $x = 0.7$; we have checked that our results are robust for x in the aforementioned range. The procedure for the KLM is similar [39].

In Fig. 1, we show the phase diagram for $t_2/t_1 = 0.25$, which reveals the three relevant phases. For small V/t_1 and J_2/J_1 the model is in the AF phase, defined by $0 < |\mathbf{M}| < 1/2$. Here, Q_{ij} is only non-zero along the vertical and horizontal bonds and $b_X = 0$. As this phase has no Kondo screening and is antiferromagnetic, we dub it AF$_S$, where the S denotes a small Fermi surface. In the limit of large frustration and small V/t_1, the model gives rise to the expected SSL-VBS, where Q_{x+y} and Q_{x-y} are the only non-zero singlet parameters. In the limit of large

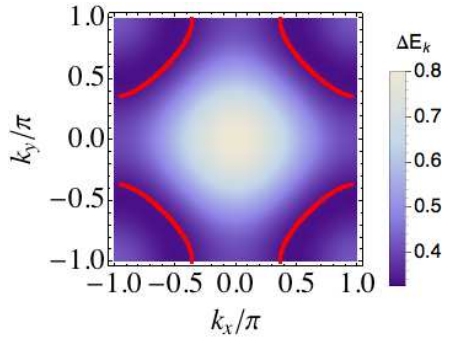

FIG. 2. (Color online). Effects of the underlying Fermi surface on the band gap in the KI phase at mixed valence. The band gap $\Delta E_{\mathbf{k}}$ is plotted in momentum space for $V/t = 2.0$ in the KI phase. The minimum of the direct band gap is along the underlying small Fermi surface (the same as for k_F with a filling $n_c \approx 1.42$), marked in red.

hybridization, all the Q_{ij} and b_X are non-zero, and they preserve the symmetry of the Shastry-Sutherland lattice. The results for the KLM are similar [39].

We find direct transitions between AF_S and KI, as well as between SSL-VBS and KI. Importantly, the notion of Kondo destruction survives the valence fluctuations inherent in the PAM [45]. While our approach yields first order transitions (see the Supplementary Material [39]), it is important to see how the fluctuation effects beyond our approach affect the nature of the transitions. Based on the studies on the quantum fluctuations in pertinent quantum impurity models [46] and Kondo lattice models [47] in the context of extended dynamical mean field approach [8, 10], we expect the transitions to be continuous.

Two remarks are in order. First, the phase diagram we have found is strikingly similar to the global phase diagram of Kondo insulators in the integer valence case proposed on qualitative grounds [27]. More generally, we can think of J_2/J_1 as a measure of the strength of quantum fluctuations in the system, and the phase diagram we have derived is representative of other means of tuning, by either frustration or dimensionality. The overall topology of the global phase diagram, consisting of two paramagnetic phases (one being KI and the other with a small Fermi surface [48]) and one AF metal phase with a small Fermi surface, is expected to be robust. Second, each type of phase transition between the KI phase and either the AF_S or the SSL-VBS is actually a *metal to insulator* transition. Thus, there should be significant effects on Fermi surface probes as the transition is approached from the metallic side as well as from the insulating side, which we now turn to.

Single-particle excitations and precursor of the small Fermi surface in the KI phase: We focus on the KI phase at mixed valence. We are primarily interested in what effects the underlying Fermi surface of the conduction electrons have "imprinted" on the properties of the insulating state. For definiteness, we will denote such small Fermi momenta by $\mathbf{k}_F$, and the large Fermi momenta that incorporate the f-electrons (see below) by $\mathbf{k}^*_F$. Note that in the mixed valence regime $\mathbf{k}_F$ is defined as the Fermi wave vector corresponding to the filling of the conduction electrons at a specific hybridization strength. To make concrete connections, we now restrict ourselves to a model defined on a 2D square lattice with NN couplings only, and therefore consider one site per unit cell. The results for integer valence in the Kondo lattice model in two and three dimensions are similar [39]. In addition, for the KI phase where the magnetic order parameter vanishes, we no longer consider the effects of the Heisenberg term in Eq. (1) and set $J_1 = J_2 = 0$; this still keeps the salient properties of the momentum distribution in this phase. Note that in the following we only have one hopping parameter t.

We first consider the hybridization gap $\Delta E_{\mathbf{k}}$ as a function of momentum in the mixed valence regime with $V/t = 2.0$, which yields a valence $n_c \approx 1.42$. Solving for the band structure in the square lattice case yields two bands $E_{\mathbf{k}\pm} = \frac{1}{2}(\epsilon_{\mathbf{k}} - \tilde{\lambda}) \pm \sqrt{\left(\frac{\epsilon_{\mathbf{k}}+\tilde{\lambda}}{2}\right)^2 + b^2}$, where $\epsilon_{\mathbf{k}} = -2t(\cos k_x + \cos k_y) - \mu$ is the dispersion with a bandwidth $W = 8t$ and chemical potential μ. A Kondo insulator of course has no Fermi surface. However, plotting the direct hybridization gap $\Delta E_{\mathbf{k}} \equiv E_{\mathbf{k}+} - E_{\mathbf{k}-}$ as a function of $\mathbf{k}$ reveals a special surface (line) in the Brillouin zone. As shown in Fig. 2, $\Delta E_{\mathbf{k}}$ is minimized along the Fermi surface of the conduction electrons marked in red, which corresponds to the small Fermi surface. We therefore reach one of our main results, namely $\Delta E_{\mathbf{k}}$ is *minimized on the small Fermi momenta,* $\mathbf{k}_F$. The magnitude of the direct and indirect gap in the integer valence limit is discussed in the Supplementary Material [39].

In addition, we consider the dispersion of the single particle excitations and momentum evolution of the conduction-electron spectral function $A(\mathbf{k}, \omega) = -\mathrm{Im}G_c(\mathbf{k}, \omega)/\pi$ [39] as shown in Fig. 3. Along the cut $k_x = k_y$ [Fig. 3(a)], we find the quasiparticle states dispersing towards the small Fermi momentum $\mathbf{k}_F \approx (0.6\pi, 0.6\pi)$ as the Fermi energy is approached, although they are eventually gapped out by the hybridization when $\mathbf{k}$ gets too close to $\mathbf{k}_F$. This point is also illustrated in the energy dispersion curves, shown in Fig. 3(c). The same trend is also observed for the momentum cut $k_y = 0$, Figs. 3 (b) and (d), for which the small Fermi momentum is never crossed.

To appreciate the above observations, we note that the small Fermi momenta $\mathbf{k}_F$ are special because, for $V = 0$ (but with $n_c \approx 1.42$), the momentum distribution of the c electrons, $n_{\mathbf{k}} = \sum_\sigma \langle c^\dagger_{\mathbf{k},\sigma} c_{\mathbf{k},\sigma}\rangle$, has a jump of exactly 1 across such momenta. A non-zero hybridization will smear this jump [38], but this smearing occurs gradually. Indeed, as shown in Fig. 4 (a), near the small Fermi

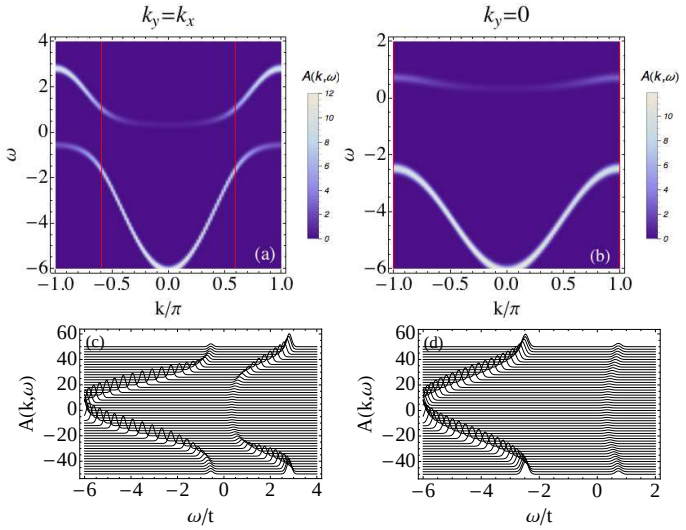

FIG. 3. (Color online). The spectral function for $V/t_1 = 2.0$ along the momentum cuts (a) $k = k_y = k_x$ and (b) $k = k_x$, $k_y = 0$. The red lines mark the location of the small Fermi momentum k_F. Energy dispersion curves of the spectral function are shown along the momentum cuts (c) $k = k_y = k_x$ and (d) $k = k_x$, $k_y = 0$. Here, each curve is shifted vertically by an integer corresponding to the wavenumber index, and we have broadened the delta function by a Gaussian of width $0.1t$.

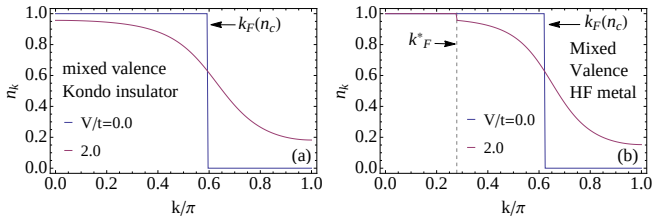

FIG. 4. (Color online). Momentum distribution of the c electrons n_k, for $k = k_x = k_y$. n_k versus k for $V/t = 2.0$ in the KI phase (a) and the metallic phase with $n_c = 1.25$ (b). The overall shape across k_F in both cases is discussed in the text, while for the metal there is a small jump at the large Fermi wave-vector k^*_F (dashed line) of the size of the quasiparticle residue.

momentum $\mathbf{k}_F$, for $V/t = 2.0$ in the KI phase, we see a step function for $V = 0$ develop into an "S-shape" pinned at $\mathbf{k}_F$. (Without a loss of generality, we focus on $0 < k_x = k_y < \pi$.) This smeared jump in the momentum distribution of the occupation number at $\mathbf{k}_F$ is caused by the same physics that induces the small excitation gap at $\mathbf{k}_F$ illustrated in Figs. 2 and 3.

The simplicity of the Kondo insulator is that the large Fermi momenta, $\mathbf{k}^*_F$, are located at the Brillouin zone boundary. This is to be contrasted with the incommensurate-filling case, as illustrated in Fig. 4(b) for $n_c = 1.25$ (corresponding to $n_c + n_d = 2.25$). In this case, the features at the small Fermi momenta, $\mathbf{k}_F$, remain similar to the Kondo insulator case. However, now, $\mathbf{k}^*_F$ occurs in the middle of the Brillouin zone. As is

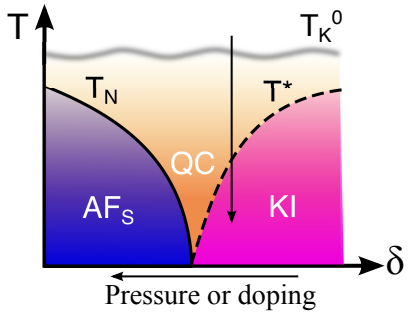

FIG. 5. (Color online). Schematic finite temperature phase diagram as a function of the control parameter δ. T^0_K is the bare Kondo temperature.)

characteristics of a heavy fermion metal [38], $n_{\mathbf{k}}$ display a tiny but sharp drop at $\mathbf{k}^*_F$.

Discussion and outlook: Several remarks are in order. Firstly, the global phase diagrams shown in Fig. 1 have a number of consequences. Tuning Kondo insulating compounds (e.g. under pressure or chemical doping, which varies the ratio of the RKKY to Kondo interactions) along some tuning-parameter trajectory opens up the exciting possibility of realizing new types of quantum phase transitions. Such a tuning can suppress the insulating gap by destroying the Kondo effect, liberate the local-moment spins, and lead to either an AF or paramagnetic metallic phase. In these metallic phases, the Fermi surface is small as defined earlier. With a continuous closure of the gap, the QCP is of the Kondo-destruction (local) type and will be interacting (instead of Gaussian).

Taking a cut in the global phase diagram leads to a schematic finite temperature phase diagram, as illustrated in Fig. 5 corresponding to the Kondo-destroyed phase nearby to the Kondo insulator being AF_S; here, both the Néel temperature T_N and the Kondo-destruction energy scale T^* go to zero at the QCP. This provides the theoretical basis to understand why pressure induces a Kondo insulator to antiferromagnetic metal transition [29–31] and why signatures of an interacting QCP such as E/T scaling will accompany such a transition.

Secondly, we have demonstrated that a precursor Fermi surface appears in a Kondo insulator, which has the form of a small Fermi surface without incorporating the f-electrons. The implications of this are significant. For example, our results imply that a Kondo insulator such as SmB_6 will have an incipient Fermi surface taking the form of the actual Fermi surface of LaB_6. Quantum oscillations have recently been extensively studied in SmB_6 [32–34], and there is evidence that the oscillation frequencies are similar to those of LaB_6 [33, 34].

In conclusion, we have determined the global phase diagram of Kondo insulators in both the periodic Anderson and Kondo-lattice models. Our result allows the under-

standing that the pressure tuning of Kondo insulators induces magnetic metal phases. Our study also underscores the simplification of the Kondo insulators compared to the heavy fermion metals, namely the absence of a (conventional) large Fermi surface. Correspondingly, our results hold the potential to open up an exciting and new direction, *viz.* to study antiferromagnetic and insulator-metal quantum phase transitions in Kondo insulators with varying geometrical frustration, or with varying dimensionality through thin films or heterostructures. Finally, we have studied the momentum distribution of the single-electron excitations in the Kondo insulator phase. We have demonstrated the imprints of a small Fermi surface in this distribution, which elucidate the recent dHvA experiments in SmB_6.

Acknowledgements: We would like to acknowledge useful discussions with D. T. Adroja, L. Balicas, S. Sebastian, F. Steglich, A. M. Strydom, L. L. Sun, and H. v. Löhneysen. This work was supported in part by JQI-NSF-PFC, LPS-MPO-CMTC, and Microsoft Q (JHP), by the National Science Foundation of China Grant number 11374361, and the Fundamental Research Funds for the Central Universities and the Research Funds of Renmin University of China (R.Y.), by the U.S. Army Research Office Grant No. W911NF-14-1-0497 and the Austrian Science Fund Grants No. I623-N16 and No. I2535-N27 (S.P.), and by the U.S. Army Research Office Grant No. W911NF-14-1-0525 and the Robert A. Welch Foundation Grant No. C-1411(Q.S.). J.H.P. acknowledges the hospitality of Rice University. J.H.P., S.P. and Q.S. acknowledge the hospitality of the Aspen Center for Physics (NSF Grant no. PHY-1066293) where this work was completed. The majority of the calculations have been performed, with support from the NSF Grant No. DMR-1309531 (Q.S.), on the Shared University Grid at Rice funded by NSF under Grant EIA-0216467, a partnership between Rice University, Sun Microsystems, and Sigma Solutions, Inc.

Note added: Upon the submission and posting of the present work, two recent theoretical studies were submitted and have since been published: O. Erten, P. Ghaemi, and P. Coleman, Phys. Rev. Lett. **116**, 046403 (2016)) and L. Zhang, X-Y Song, and F. Wang, Phys. Rev. Lett. **116**, 046404 (2016); the motivations of these studies in part overlap with those of ours.

[1] H. v. Löhneysen, Special issue on Quantum Phase Transitions, J. Low Temp. Phys. **161**, 1 (2010).
[2] Q. Si and F. Steglich, Science **329**, 1161 (2010).
[3] H. v. Löhneysen, A. Rosch, M. Vojta, and P. Wölfle, Rev. Mod. Phys. **79**, 1015 (2007).
[4] A. Schröder, G. Aeppli, R. Coldea, M. Adams, O. Stockert, H. v. Löhneysen, E. Bucher, R. Ramazashvili, and P. Coleman, Nature **407**, 351 (2000).
[5] S. Paschen, T. Lühmann, S. Wirth, P. Gegenwart, O. Trovarelli, C. Geibel, F. Steglich, P. Coleman, and Q. Si, Nature **432**, 881 (2004).
[6] H. Shishido, R. Settai, H. Harima, and Y. Ōnuki, Journal of the Physical Society of Japan **74**, 1103 (2005).
[7] S. Friedemann, N. Oeschler, S. Wirth, C. Krellner, C. Geibel, F. Steglich, S. Paschen, S. Kirchner, and Q. Si, Proceedings of the National Academy of Sciences **107**, 14547 (2010).
[8] Q. Si, S. Rabello, K. Ingersent, and J. L. Smith, Nature **413**, 804 (2001).
[9] P. Coleman, C. Pépin, Q. Si, and R. Ramazashvili, Journal of Physics: Condensed Matter **13**, R723 (2001).
[10] Q. Si, J. H. Pixley, E. Nica, S. J. Yamamoto, P. Goswami, R. Yu, and S. Kirchner, Journal of the Physical Society of Japan **83**, 061005 (2014).
[11] M. S. Kim and M. C. Aronson, Phys. Rev. Lett. **110**, 017201 (2013).
[12] D. D. Khalyavin, D. T. Adroja, P. Manuel, A. Daoud-Aladine, M. Kosaka, K. Kondo, K. A. McEwen, J. H. Pixley, and Q. Si, Phys. Rev. B **87**, 220406 (2013).
[13] E. D. Mun, S. L. Bud'ko, C. Martin, H. Kim, M. A. Tanatar, J.-H. Park, T. Murphy, G. M. Schmiedeshoff, N. Dilley, R. Prozorov, and P. C. Canfield, Phys. Rev. B **87**, 075120 (2013).
[14] V. Fritsch, N. Bagrets, G. Goll, W. Kittler, M. J. Wolf, K. Grube, C.-L. Huang, and H. v. Löhneysen, Phys. Rev. B **89**, 054416 (2014).
[15] Y. Tokiwa, C. Stingl, M.-S. Kim, T. Takabatake, and P. Gegenwart, Science Advances **1**, e1500001 (2015).
[16] J. Custers, K. A. Lorenzer, M. Müller, A. Prokofiev, A. Sidorenko, H. Winkler, A. M. Strydom, Y. Shimura, T. Sakakibara, R. Yu, and et. al., Nature materials **11**, 189 (2012).
[17] S. Friedemann, T. Westerkamp, M. Brando, N. Oeschler, S. Wirth, P. Gegenwart, C. Krellner, C. Geibel, and F. Steglich, Nature Physics **5**, 465 (2009).
[18] J. Custers, P. Gegenwart, C. Geibel, F. Steglich, P. Coleman, and S. Paschen, Phys. Rev. Lett. **104**, 186402 (2010).
[19] L. Jiao, Y. Chen, Y. Kohama, D. Graf, E. Bauer, J. Singleton, J.-X. Zhu, Z. Weng, G. Pang, T. Shang, *et al.*, Proceedings of the National Academy of Sciences **112**, 673 (2015).
[20] Q. Si, Physica B: Condensed Matter **378**, 23 (2006).
[21] Q. Si, Physica Status Solidi (b) **247**, 476 (2010).
[22] P. Coleman and A. H. Nevidomskyy, Journal of Low Temperature Physics **161**, 182 (2010).
[23] J. H. Pixley, R. Yu, and Q. Si, Phys. Rev. Lett. **113**, 176402 (2014).
[24] Q. Si and S. Paschen, physica status solidi (b) **250**, 425 (2013).
[25] G. Aeppli and Z. Fisk, Comments Cond. Mat. Phys. **16**.
[26] P. S. Riseborough, Advances in Physics **49**, 257 (2000).
[27] S. J. Yamamoto and Q. Si, Journal of Low Temperature Physics **161**, 233 (2010).
[28] M. Dzero, K. Sun, V. Galitski, and P. Coleman, Phys. Rev. Lett. **104**, 106408 (2010).
[29] Y. Zhou, Q. Wu, P. F. S. Rosa, R. Yu, J. Guo, W. Yi, S. Zhang, Z. Wang, S. Wang, Honghong abd Cai, K. Yang, A. Li, Z. Jiang, S. Zhang, X. Wei, Y. Huang, Y.-f. Yang, Z. Fisk, Q. Si, L. Sun, and Z. Zhao, (2016), arXiv:1603.05607.
[30] A. Barla, J. Derr, J. P. Sanchez, B. Salce, G. Laper-

tot, B. P. Doyle, R. Rüffer, R. Lengsdorf, M. M. Abd-Elmeguid, and J. Flouquet, Phys. Rev. Lett. **94**, 166401 (2005).
[31] S. Gabáni, E. Bauer, S. Berger, K. Flachbart, Y. Paderno, C. Paul, V. Pavlík, and N. Shitsevalova, Phys. Rev. B **67**, 172406 (2003).
[32] G. Li, Z. Xiang, F. Yu, T. Asaba, B. Lawson, P. Cai, C. Tinsman, A. Berkley, S. Wolgast, Y. S. Eo, *et al.*, Science **346**, 1208 (2014).
[33] B. Tan, Y.-T. Hsu, B. Zeng, M. C. Hatnean, N. Harrison, Z. Zhu, M. Hartstein, M. Kiourlappou, A. Srivastava, M. Johannes, *et al.*, Science **349**, 287 (2015).
[34] M. Hartstein *et al.*, preprint (2016).
[35] D. Baumgartner, "Crystal growth and physical properties of the heavy fermion system $CeCu_xNi_{1-x}Sn$ near a quantum critical point", Diploma thesis, Vienna University of Technology, (2015).
[36] D. Adroja et al, work presented at ICM 2015 (July, 2015, Barcelona).
[37] W. T. Fuhrman *et al.*, private communications (2015).
[38] A. C. Hewson, *The Kondo problem to heavy fermions*, 2 (Cambridge university press, 1997).
[39] See Supplementary Material at:.
[40] B. H. Bernhard, B. Coqblin, and C. Lacroix, Phys. Rev. B **83**, 214427 (2011).
[41] B. H. Bernhard and C. Lacroix, Phys. Rev. B **92**, 094401 (2015).
[42] B. S. Shastry and B. Sutherland, Physica B+ C **108**, 1069 (1981).
[43] S. Miyahara and K. Ueda, Journal of Physics: Condensed Matter **15**, R327 (2003).
[44] J. W. Negele and H. Orland, *Quantum Many-Particle Systems* (Westview Press, Boulder, CO, 1998).
[45] In the incommensurate-filling case [23], there are various intermediate phases (between the VBS and heavy Fermi liquid) that break the underlying symmetry of the Shastry-Sutherland lattice and as a result exhibit partial Kondo screening. Here, we find these solutions to be energetically not competitive.
[46] E. M. Nica, K. Ingersent, J.-X. Zhu, and Q. Si, Phys. Rev. B **88**, 014414 (2013).
[47] E. M. Nica, K. Ingersent, and Q. Si, (2016), arXiv:1603.03829.
[48] S. J. Yamamoto and Q. Si, Phys. Rev. Lett. **99**, 016401 (2007).